

# Quantifying the Stress Relaxation Modulus of Polymer Thin Films via Thermal Wrinkling

Edwin P. Chan,<sup>†</sup> Santanu Kundu,<sup>†</sup> Qinghuang Lin,<sup>‡</sup> and Christopher M. Stafford<sup>\*†</sup>

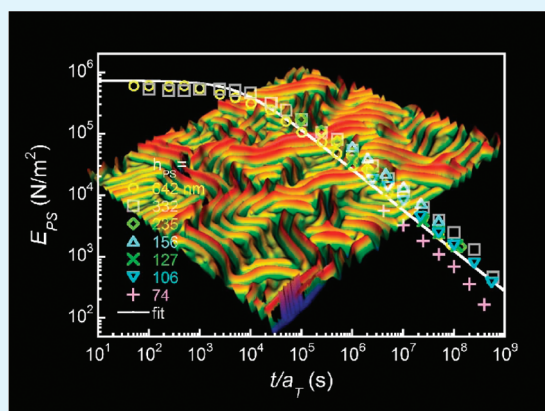
<sup>†</sup>Polymers Division, National Institute of Standards and Technology, 100 Bureau Drive, Gaithersburg, Maryland 20899, United States

<sup>‡</sup>IBM T. J. Watson Research Center, P.O. Box 218, Yorktown Heights, New York 10598, United States

## S Supporting Information

**ABSTRACT:** The viscoelastic properties of polymer thin films can have a significant impact on the performance in many small-scale devices. In this work, we use a phenomenon based on a thermally induced instability, termed thermal wrinkling, to measure viscoelastic properties of polystyrene films as a function of geometric confinement via changes in film thickness. With application of the appropriate buckling mechanics model for incompressible and geometrically confined films, we estimate the stress-relaxation modulus of polystyrene films by measuring the time-evolved wrinkle wavelength at fixed annealing temperatures. Specifically, we use time-temperature superposition to shift the stress relaxation curves and generate a modulus master curve for polystyrene films investigated here. On the basis of this master curve, we are able to identify the rubbery plateau, terminal relaxation time, and viscous flow region as a function of annealing time and temperatures that are well-above its glass transition. Our measurement technique and analysis provide an alternative means to measure viscoelastic properties and relaxation behavior of geometrically confined polymer films.

**KEYWORDS:** polystyrene, viscoelastic properties, thin films, wrinkling, stress relaxation modulus



## 1. INTRODUCTION

Polymer multilayer films are ubiquitous in many important technological applications that include electronics,<sup>1–3</sup> photonics,<sup>4</sup> optics,<sup>5</sup> and energy storage.<sup>6</sup> In these applications, the viscoelastic properties of the polymer layers play a key role in device performance. For example, in organic transistors,<sup>2</sup> the viscoelastic properties of an underlying polymer gate dielectric layer can change the morphology of an organic semiconductor material, thus affecting transistor performance of the semiconductor material. For non-volatile memory storage, the temperature-dependent mechanical properties of the polymer thin film as well as the relaxation time for reflow are critical to the write/rewrite speed of the memory device.<sup>3</sup> In photonic crystal multilayers, the shear viscosity of the polymer layers affects the uniformity of the layer dimensions during processing,<sup>4</sup> which would affect the optical properties of the final structure. These examples indicate the importance of measuring the viscoelastic properties for polymer thin films. For bulk polymers with macroscopic film dimensions, measuring or predicting their viscoelastic properties is relatively straightforward. However, these properties do not necessarily translate to the thin film analogs. As research over the past decade has suggested, the mechanical properties of polymer thin films are unique because their properties are quite sensitive to the changes in the interfacial

properties such as film thickness, as well as interfacial energies at the substrate and superstrate. Unfortunately, it is quite challenging to adapt bulk polymer measurement approaches for polymer thin films. Therefore, there has been a drive to develop measurement techniques that can probe the viscoelastic properties of polymer thin films.<sup>7–12</sup>

One of the earliest attempts to measure the viscous properties of a polymer thin film was polymer thin film dewetting.<sup>7,12</sup> By allowing a thin, liquid-like polymer film to dewet and form holes from a nonwetting substrate, the viscosity of the polymer layer can be inferred based on the growth rate of the holes. To quantify the elastic properties of polymer thin films, researchers developed nanobubble inflation that infers the creep compliance of a polymer thin film by measuring its resistance to inflate into a dome.<sup>10</sup> Both of these techniques are novel for their simplicity in probing the viscoelastic properties of polymer thin films. More intricate measurement approaches such as indentation,<sup>9</sup> dielectric spectroscopy,<sup>8</sup> and acoustic impedance<sup>11</sup> have been developed that can probe both the elastic and viscous properties of polymer thin films. However, as most of these approaches are dealing with the

**Received:** October 4, 2010

**Accepted:** December 13, 2010

**Published:** December 29, 2010

**Table 1. Summary of Material Properties of Aluminum (Al), Polystyrene (PS), and Silicon (Si), Including Film Thickness ( $h_i$ ), Elastic Modulus ( $E_i$ ), Poisson's Ratio ( $\nu_i$ ), and Thermal Expansion Coefficient ( $\alpha_i$ )<sup>a</sup>**

	$h_i$ (nm)	$E_i$ (N/m <sup>2</sup> )	$\nu_i$	$\alpha_p$ (1/°K)
Al	21	$7.0 \times 10^{10}$	0.33	$2.3 \times 10^{-5}$
PS	$74 \pm 1, 106 \pm 1, 127 \pm 1, 156 \pm 1, 235 \pm 1, 332 \pm 2, 642 \pm 4$		0.5 0.33	$(T \geq T_g) 1.7 \times 10^{-4}$ $(T < T_g) 5.7 \times 10^{-5}$
Si	$5 \times 10^{-5}$	$1.8 \times 10^{11}$	0.2	$5.5 \times 10^{-6}$

<sup>a</sup> The thermal expansion coefficients for Al and Si were taken from Kim and Lee,<sup>14</sup> and the thermal expansion coefficients for PS was taken from Wallace et al.<sup>39</sup> The elastic modulus and Poisson's ratio for Al were taken from Zhang et al.<sup>18</sup> The elastic modulus and Poisson's ratio for Si was taken from Kim.<sup>40</sup>

viscoelastic properties of polymer thin films in contact with a free surface, the contributions of air–polymer surface energy to the interpretation of the results must be considered. Additionally, the geometry of many polymer thin film applications is in the form of a multilayer structure. Therefore, it would be desirable to have a measurement approach that can easily probe the viscoelastic properties of a polymer thin film sandwiched between a substrate and a superstrate.

Recently, we have developed a new method to probe the viscoelastic properties of polymer thin films using thermal wrinkling of an aluminum-capped polymer thin film at elevated temperatures.<sup>13</sup> This approach takes advantage of a thermally induced instability that develops in a trilayer film (i.e., polymer film sandwiched between stiffer substrate and superstrate layers) with different thermal expansion coefficients ( $\alpha$ ).<sup>14–24</sup> This approach is relevant to trilayers where the substrate has the lowest thermal expansion. In these systems, a net compressive strain develops at the polymer–superstrate interface when annealed at elevated temperatures. At a sufficiently high annealing temperature where a critical compressive strain for wrinkling is reached, surface wrinkles develop on the superstrate surface and can be characterized by an isotropic morphology having a sinusoidal surface profile. By monitoring the time-evolution of the wrinkle wavelength and amplitude, we can infer viscoelastic properties of the polymer layer with the use of appropriate buckling mechanics relationships.

In this work, we investigate the role of geometric confinement, via changes in polymer film thickness, on the thermal wrinkling process and the viscoelastic properties of aluminum-capped polystyrene thin films. We refine our previous model and improve the interpretation of the wrinkle wavelength evolution. With the appropriate buckling mechanics relationships that consider the deformation of geometrically confined and incompressible films, we are able to quantify the stress-relaxation modulus and relaxation time for these materials. Specifically, we apply the principle of time–temperature superposition to time-shift the stress relaxation curves and generate a modulus master curve for polystyrene films investigated here. Using this approach, we are able to identify the rubbery plateau, the terminal relaxation time, along with the viscous flow regime of the polystyrene thin films as a function of annealing time and annealing temperature range well-above the glass transition.

## 2. EXPERIMENTAL SECTION

**General.** Certain commercial equipment, instruments, or materials are identified in this paper in order to specify the experimental procedure adequately. Such identification is not intended to imply recommendation or endorsement by the National Institute of Standards and Technology, nor is it intended to imply that the materials or equipment identified are necessarily the best available for the purpose. The error bars represent one standard deviation of the data, which is taken as the uncertainty of the measurement.

**Materials.** We chose monodisperse polystyrene (PS) homopolymer (mass average molecular mass of 106 000 g/mol, polydispersity of 1.05, Polymer Source) as our model polymer thin film. This molecular mass was selected because it is well above its entanglement molecular mass, which facilitates the existence of a rubbery plateau and viscous flow regions. Hence, we can use thermal wrinkling to probe different regions of the elastic and viscous response of PS at the annealing temperatures investigated.

PS thin films on silicon substrates were prepared by spin-coating 2–10% by mass toluene (anhydrous, 99.8%, Sigma-Aldrich) PS solutions onto UVO-cleaned (5 min, model 342, Jelight Company) Si substrates. The films were then annealed at 125 °C for 24 h. The thicknesses of the PS thin films ( $h_{PS}$ ) were measured by interferometry (Model F20, Filmetrics, Inc.). Aluminum (Al) was then deposited by thermal evaporation and the thickness ( $h_{Al}$ ) was kept constant at 21 nm for all PS samples. The thickness of the Al layer must be sufficiently thin to facilitate wrinkling because the critical strain to cause thermal wrinkling is proportional to its thickness for geometrically confined systems. We selected this Al film thickness as we found that films below this thickness to be less reflective, which would lead to a reduction in signal detection during the subsequent small-angle laser light scattering experiments. These composite films were used for thermal wrinkling measurements without further processing. Table 1 summarizes the PS film thicknesses investigated in this study.

**Thermal Wrinkling.** The thermal wrinkling experiments were conducted with a custom-built instrument as described previously (Figure 1).<sup>13</sup> A thermal wrinkling experiment was carried out in the following manner. The hot-stage (Linkam TMS94, Linkam Scientific Instruments, Ltd.) was heated to a predetermined annealing temperature ( $T$ ). The annealing temperatures ranged from 120 to 170 °C depending on the specific PS film thickness tested. Temperatures at the polymer substrate were monitored throughout the experiment, with a variation of less than 0.3 °C during the experiment. Once  $T$  was stable, a 1 cm × 1 cm specimen of the trilayer film was placed onto the heated hot-stage for an annealing time of at least 3600 s. Over the course of this annealing time ( $t$ ), wrinkles developed on the aluminum film surface. We used small-angle laser light scattering to monitor the isothermal changes of the wrinkle wavelength and amplitude as a function of  $t$ . The two-dimensional (2D) scattering patterns were collected with a CCD camera (Apogee kx260e, Apogee Instruments, Inc.), which is controlled via a custom-designed National Instruments LabVIEW interface.

A representative thermal wrinkling experiment is shown in panels b and c in Figure 1. At an annealing time of 0 s, the scattering profiles are featureless with relatively low intensity, which is indicative of an initially smooth Al surface. Because wrinkle formation is related to the thermal properties of the trilayer film, we attribute this observation to the development of a thermal mismatch strain below the critical value for wrinkle initiation. As annealing time progresses, sufficient thermal strain builds up within the trilayer and wrinkles begin to develop. Figure 1b illustrates the scattering pattern for isotropic wrinkles, which is characterized as a halo pattern with a dominant wavelength ( $d$ ) at the maximum scattering intensity ( $I$ ). Each image was analyzed via another custom-designed National Instruments LabVIEW interface that performs an azimuthal averaging of the 2D pattern into a 1D plot of scattering intensity ( $I$ ) vs scattering vector ( $k$ ). From this plot, we interpolate the  $k$  at

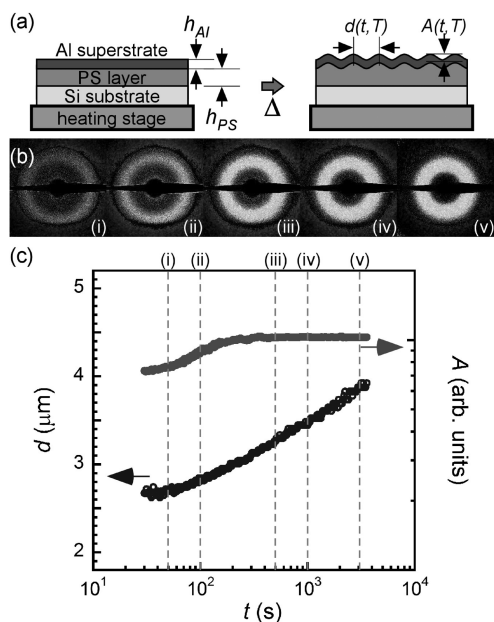


**Figure 1.** Thermal wrinkling approach of a PS thin film. (a) The PS layer is sandwiched between an Al superstrate and a Si substrate. (b) Representative 2D scattering patterns for a 332 nm thick PS film isothermally annealed at 140 °C as a function of annealing time ( $t$ ). (c) Evolution of the wrinkle wavelength ( $d$ ) and amplitude ( $A$ ) as a function of annealing time at 140 °C.

maximum  $I$ , with the aid of a Gaussian curve fitting routine, and convert the values into real space parameters of wavelength ( $d = 2\pi/k$ ) and amplitude ( $A \approx I^{1/2}$ ).<sup>25</sup>

**Thermal Wrinkling As a Measurement Tool.** The formation of surface wrinkles on the Al superstrate is associated with a net compressive strain that develops due to the thermal expansion mismatch between the layers. At a given  $T$ , each layer will expand laterally by an amount of thermal strain ( $\epsilon_i$ ) defined by  $\epsilon_i = \alpha_i \Delta T$  (Figure 2a). For our materials (Table 1), we expect that the PS layer will expand the most, followed by Al and then Si. Because the expansions of the layers are coupled with each other due to adhesion at the interfaces, strain compatibility condition must be satisfied at all of these interfaces. Both the PS and Al layers will experience net compressive strains of  $\epsilon_{T,Al}$  and  $\epsilon_{T,PS}$  as their thermal expansions must be consistent with that of the rigid Si substrate.<sup>26</sup> On the basis of the thin film approximation, we define the magnitude of these compressive strains by the following

$$\epsilon_{T,Al} = -(\alpha_{Si} - \alpha_{Al})(T - T_{RT}) \quad (1)$$

$$\epsilon_{T,PS} = -(\alpha_{Si} - \alpha_{PS, T < T_g})(T_g - T_{RT}) + (\alpha_{Si} - \alpha_{PS, T \geq T_g})(T - T_g) \quad (2)$$

If the deformations are assumed to be linear elastic, then the thermal stress is directly related to the thermal strain by the plane-stress elastic modulus ( $E_i/(1 - \nu_i)$ ). Figure 2b quantifies the amount of thermal strain experienced by the Al and PS layers as a function of the annealing temperatures investigated, demonstrating that the compressive strain is below the yield strain of Al ( $\approx 0.4\%$ ).<sup>27</sup>

On the basis of linear stability analysis, the critical strain for wrinkling ( $\epsilon_w$ ) of the Al thin film supported by a semi-infinitely thick PS layer is related to the elastic modulus and Poisson's ratio of the PS ( $E_{PS}$ ,  $\nu_{PS}$ ) and Al ( $E_{Al}$ ,  $\nu_{Al}$ ) layers, respectively<sup>28</sup>

$$\epsilon_w = \frac{1}{4} \left( 3 \frac{E_{PS}}{1 - \nu_{PS}^2} \frac{1 - \nu_{Al}^2}{E_{Al}} \right)^{2/3} \quad (3)$$

Thermal wrinkling occurs when  $\epsilon_{T,Al} \geq \epsilon_w$ . If the material properties of the Al and PS are known, we can then determine the critical temperature for wrinkling ( $T_c$ ) by comparing eq 1 and eq 3.

To take advantage of thermal wrinkling as a measurement tool, we need to identify the range of  $E_{PS}$  values that can be accessed. Specifically, the critical modulus ( $E_{PS,c}$ ) can be determined as a function of  $T_c$  by comparing eqs 1 and 3.

$$E_{PS,c}^* = \frac{E_{PS,c}}{1 - \nu_{PS}^2} = \frac{8}{3} \left( \frac{E_{Al}}{1 - \nu_{Al}^2} \right) [(\alpha_{Al} - \alpha_{Si})(T_c - T_{RT})]^{3/2} \quad (4)$$

Substituting the materials properties of Table 1 into eq 4, we can determine  $E_{PS,c}$  as a function of  $T_c$  (Figure 2c). This plot identifies the measurement threshold of thermal wrinkling in determining  $E_{PS}$ . Elastic modulus values above the  $E_{PS,c}$  curve cannot be measured because there is insufficient thermal strain to cause wrinkling. Hence, the trilayer film will appear flat even though the trilayer is thermally strained at these annealing temperatures. Conversely, the region below this curve defines the envelope where there is sufficient thermal strain to cause wrinkling. Hence, the elastic modulus of PS must fall within this window to be measurable by thermal wrinkling. Additionally, we note that this envelope will decrease when the thickness of the PS film affects the wrinkling process. As we will discuss in the next section, this change is associated with the increased resistance of the trilayer to undergo thermal wrinkling.

**Relationships between Wavelength, Film Thickness, And Modulus.** Since we infer the PS modulus using thermal wrinkling, it is critical that we understand the relationships between wrinkle wavelength, film thickness and material property. The dimensionless membrane force links the wrinkle wavelength to the materials properties of the Al and PS and is defined by<sup>19</sup>

$$f = \frac{(kh_{Al})^2}{12} + \frac{g(kh_{PS}, \nu_{PS})}{(kh_{Al})} \frac{E_{PS}(1 - \nu_{Al}^2)}{E_{Al}(1 - \nu_{PS}^2)} \quad (5)$$

where  $g(kh_{PS}, \nu_{PS})$  is a dimensionless stiffness function related to the thickness and Poisson's ratio of PS. The parameter reciprocal wavelength,  $k = 2\pi/d$ , with  $h_{Al}$  and  $h_{PS}$  corresponding to the thickness of the Al and PS, respectively. For polymer films where the Poisson's ratio is significantly far from incompressible (i.e.,  $\nu = 0.33$ ), solutions for the stiffness function have been developed that relates the wrinkle wavelength to the material properties of the polymer layer.<sup>29</sup> When the PS can be considered as incompressible ( $\nu_{PS} = 0.5$ ), a unique solution exists for the stiffness function where the explicit relationship between the wrinkling wavelength and PS film thickness depend on the extent of geometric confinement of the wrinkling process. Relationships between  $kh_{Al}$  and  $g(kh_{PS}, \nu_{PS})$  are provided in the Supporting Information, section S1.

$$g(kh_{PS}, \nu_{PS} = 0.5) = \frac{1}{2} \frac{\cosh(2kh_{PS}) + 2(kh_{PS})^2 + 1}{\sinh(2kh_{PS}) - 2(kh_{PS})} \quad (6)$$

Since the annealing temperatures were above the PS glass-transition temperature ( $T_g \approx 105$  °C), we assume that the PS is behaving as primarily elastic at short times with the presence of cross-links because of physical entanglements of the polymer chains whose molecular mass is above the entanglement limit. On the basis of this assumption, we considered the PS to be incompressible. Unlike a chemically cross-linked rubber with a fixed number of cross-links per volume, the entanglements for PS consist of physical associations whose density decrease with annealing temperature. Thus, we would expect that this decrease in entanglement density would change  $\nu_{PS}$  with annealing temperature. However, as measuring the exact value of the Poisson's ratio is nontrivial, we chose a constant value ( $\nu_{PS} = 0.5$ ) at all the annealing temperatures investigated. By minimizing eq 5 with respect to  $k$ , the specific relationships between modulus and wrinkle wavelength can be established since

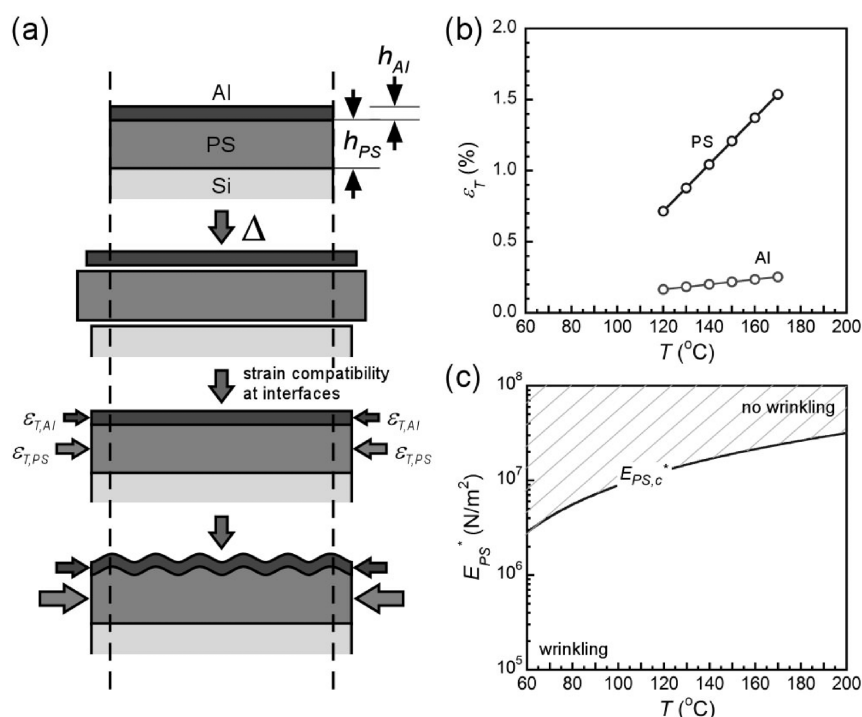


**Figure 2.** Mechanism of thermal wrinkling. (a) Schematic of the thermal expansion process and the resultant net compression of the Al and PS layers. (b) Calculated thermal strains ( $\epsilon_T$ ) for the Al and PS layers based on eq 1 and eq 2. (c) Plane strain elastic modulus of PS ( $E_{PS}^*$ ) accessible by thermal wrinkling as a function of annealing temperature ( $T$ ). The curve defines the critical value of  $E_{PS}^*$  ( $E_{PS,c}^*$ ) below which the thermal wrinkling occurs. The room temperature ( $T_{RT}$ ) is 25 °C.

this stiffness function captures the changes in wrinkle wavelength due to changes in the bending stiffness of the PS layer.

The combination of eq 5 and eq 6 defines two limiting cases that are important. The first is the “geometrically unconfined” limit where the PS film thickness is greater than the wrinkle wavelength. If the PS layer is considered as infinitely thick in comparison to the thin Al layer ( $h_{PS} > 100h_{Al}$ ), then eq 6 is independent of the PS film thickness and  $g(kh_{PS} = \infty, \nu_{PS} = 0.5) = 1/2$ . By minimizing eq 5, the elastic modulus of the PS layer is related to  $k$ , thus the wrinkle wavelength, by the following relationship.

$$E_{PS}(kh_{PS} \rightarrow \infty) = \frac{E_{Al}(1 - \nu_{PS}^2)}{3(1 - \nu_{Al}^2)} (kh_{Al})^3 \quad (7)$$

Equation 7 is a well-established expression<sup>28,30,31</sup> relating the elastic modulus of the PS film to the measured wrinkle wavelength ( $d = 2\pi/k$ ), thickness of the Al film ( $h_{Al}$ ), and elastic modulus of the Al superstrate ( $E_{Al}$ ). It assumes that the PS film is sufficiently thick such that the wrinkle wavelength is only dependent on  $h_{Al}$ .

The second case is the “geometrically confined” limit where the PS film thickness is less than the wrinkle wavelength. Here, the PS film thickness becomes commensurate with the Al thickness ( $h_{PS} < 100h_{Al}$ ). In this limit, the specific relationship between wavelength and material properties is highly dependent on the Poisson's ratio of the polymer layer because the Poisson's ratio describes the ability for the layer to relieve the compressive strain by wrinkling. For our materials, eq 6 now becomes  $g(kh_{PS} \rightarrow 0, \nu_{PS} = 0.5) = (3/4)(kh_{PS})^{-3}$ . Minimization of eq 5 yields

$$E_{PS}(kh_{PS} \rightarrow 0) = \frac{E_{Al}}{18(1 - \nu_{Al}^2)} \left(\frac{h_{PS}}{h_{Al}}\right)^3 (kh_{Al})^6 \quad (8)$$

Physically, eq 8 accounts for the effect of decreasing film thickness in increasing the resistance of the PS layer to thermally wrinkle. The ratio of PS and Al thickness captures this stiffening effect since the critical

compressive strain for wrinkling now scales with  $(h_{Al}/h_{PS})$ .

$$\epsilon_w = \frac{1}{4} \left(\frac{h_{Al}}{h_{PS}}\right) \left(3E_{PS} \frac{1 - \nu_{Al}^2}{E_{Al}}\right)^{1/3} \quad (9)$$

In other words, the minimal compressive strain required for wrinkling increases as the PS film thickness decreases. We note that eq 8 is valid only if the PS is considered to be incompressible. If the PS is compressible, i.e., when the annealing temperature is below the glass transition, then the Winkler model is more appropriate in describing the modulus of PS.<sup>19,32</sup>

If the elastic modulus is independent of testing history such as annealing time and temperature, then the thermal wrinkling measurement is straightforward because a single thermal wrinkling experiment at a single annealing temperature is required to determine PS elastic modulus. However, most polymers including PS are viscoelastic materials. This implies that their mechanical properties must be measured as a function of both annealing time and temperature. As we will demonstrate, thermal wrinkling provides an indirect probe to measure the modulus and relaxation time of the PS layer by monitoring the changes in the wrinkle wavelength and amplitude as a function of annealing time and temperature. Additionally, we kept the Al film thickness constant and only varied the PS, which allows us to monitor the properties of the PS layer as a function of film thickness.

**Bulk Rheology.** For comparison of our thermal wrinkling results, we measured the viscoelastic properties of a bulk PS sample using parallel plate rheometry. The dynamic rheological experiments were conducted on an ARES-LS rheometer (TA Instruments). The experiments were performed over a temperature range of 130 to 160 °C at 10 °C interval using 25 mm parallel plate fixtures. The gap thickness was maintained at 1 mm in all the tests. All frequency sweep data were collected at strain amplitude of 0.1% to 0.3% strain, which is within the linear viscoelastic regime of PS. Time-temperature superposition results for the storage modulus are provided in the Supporting Information S2 for a frequency range from  $1 \times 10^{-6}$  rad/s to  $1 \times 10^1$  rad/s.

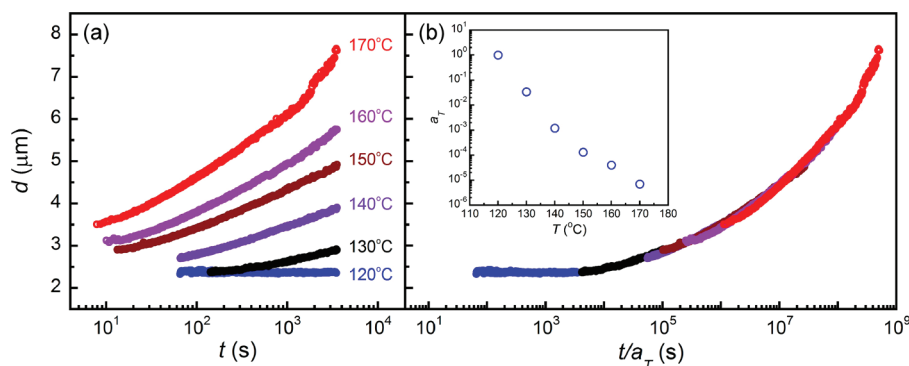


**Figure 3.** (a) Evolution of the wrinkle wavelength ( $d$ ) for a 332 nm thick PS film as a function of annealing time ( $t$ ) and temperature ( $T$ ). (b) Wrinkle wavelength modulus master curve for a 332 nm thick PS film based on time–temperature superposition of the results in (a). The inset summarizes the shift factors ( $a_T$ ) used for the annealing time shift. The error bars are smaller than the symbol size.

### 3. RESULTS AND DISCUSSION

#### Effects of Viscoelastic Properties on Thermal Wrinkling.

Once the critical strain for wrinkling develops, the wavelength should remain constant because it is strain-independent past this critical point. As shown in Figure 2b, the compressive strain due to thermal mismatch is below the yield point of Al. Assuming that the Al layer is experiencing elastic deformations at these annealing temperatures, we would expect that wavelength is independent of both annealing time and temperature. Hence, eqs 7 and eq 8 should be sufficient in predicting the elastic modulus of the PS layer.

However, it is well-established that PS is viscoelastic at the annealing temperatures investigated. Therefore, the wrinkle wavelength should not be a constant value, but rather it should depend on the annealing time and temperature because the modulus of PS is changing under these conditions. As we have assumed that a constant compressive strain is applied to the PS layer due to thermal mismatch, changes in the wrinkle wavelength reflect the changes in the properties of the viscoelastic PS layer. In other words, a thermal wrinkling experiment measures the stress relaxation modulus of the PS layer. If we consider the thermal wrinkling of a 332 nm thick PS film (Figure 3a), the wrinkle wavelength changes significantly and depends on both annealing time and temperature. More importantly, this response is consistently observed for all the PS film thicknesses.

The lowest annealing temperature to observe wrinkling was  $T = 120$  °C. We note that this temperature is not the lowest annealing temperature to cause wrinkling but it represents the lowest that can be resolved by the SALS instrument. At this temperature, the wrinkle wavelength was insensitive to the annealing time as indicated by the constant value. With increasing annealing temperature, the wrinkle wavelength increased nonlinearly with annealing time. In evaluating the wrinkle wavelength at short times versus annealing temperature, we found that the initial wavelength increases with annealing temperature. All of these results indicated that mechanical properties of PS are sensitive to both annealing time and temperature. Hence, eq 7 and eq 8 must be re-evaluated to account for this time- and temperature-dependent modulus of PS ( $E_{PS}(t, T)$ ). To account for viscoelastic effects, eq 7 and eq 8 become

$$E_{PS}(t, T, kh_{PS} \rightarrow \infty) = \frac{E_{Al}(1 - \nu_{PS}^2)}{3(1 - \nu_{Al}^2)} (k(t, T)h_{Al})^3 \quad (10)$$

$$E_{PS}(t, T, kh_{PS} \rightarrow 0) = \frac{E_{Al}}{18(1 - \nu_{Al}^2)} \left(\frac{h_{PS}}{h_{Al}}\right)^3 (k(t, T)h_{Al})^6 \quad (11)$$

**Wrinkle Wavelength Master Curve.** For a specific annealing time at a given annealing temperature, the wavelength was equivalent to the value obtained at a different annealing time and annealing temperature. This time–temperature equivalence in the wrinkle wavelength, which is related to the modulus of PS, is similar to the response that observed in bulk rheological testing of PS. In bulk testing of rheologically simple polymers, time–temperature superposition<sup>33</sup> is often used to greatly reduce experimental time as the approach can map the modulus over many decades of time by time-shifting modulus measurements obtained at different temperatures to a common reference temperature.

We used this time–temperature superposition approach to establish a wavelength master curve to link all the wavelength–time curves at different annealing temperatures. The approach is based on the premise that the wavelength is related to the modulus of the polymer layer in a predictive manner as presented above. The master curve for the 332 nm thick PS film is shown in Figure 3b. To assemble this master curve, we took the wavelength–time curve measured at each annealing temperature and horizontally shifted each curve with respect to a reference temperature ( $T_R$ ). Each curve was time-shifted by a unique shift factor ( $a_T$ ) that was empirically determined by matching equivalent wavelength values to determine average shift constants for the entire curve. We chose a reference temperature  $T_R = 120$  °C as it was the lowest annealing temperature where thermal wrinkling can be resolved by SALS. Shift factors determined for each annealing temperature are shown in the inset of Figure 3b. The constants of  $C_1$  and  $C_2$  can be determined using the well-established Williams–Landau–Ferry (WLF) equation<sup>34</sup>

$$\log a_T = \frac{-C_1(T - T_R)}{C_2 + (T - T_R)} \quad (12)$$

Substituting the shift factors into eq 12 at the appropriate annealing temperatures ( $T$ ), we determined shift constants,  $C_1 = 9.87$  and  $C_2 = 47.3$  K fit our data, which is in close agreement to reported values.<sup>35</sup>

**Wavelength Master Curve As a Function of PS Film Thickness.** Resolving the wrinkle wavelength with SALS became more challenging as we reduced the PS film thickness. This difficulty is attributed to the reduced signal-to-noise ratio of the

scattering intensity with reducing PS film thickness. Because the intensity is related to the wrinkle amplitude, this decrease in signal is again attributed to the increased stiffness of the PS layer with decreasing thickness since the wrinkle amplitude scales with the critical compressive strain as  $A \approx (\varepsilon_w)^{-1/2} \approx (h_{AI}/h_{PS})^{-1/2}$ . This prediction was experimentally confirmed as we found that the critical wrinkling temperature increased with decreasing film thickness. Although the 642 and 332 nm thick PS thermally wrinkled at  $T = 120^\circ\text{C}$ , the remaining samples wrinkled at higher annealing temperatures. In general, the annealing temperature when wrinkling was observed by SALS increased with decreasing film thickness. To generate wavelength master curves for each film thickness using time–temperature superposition, we used the shift factors determined from the 642 nm PS film (inset in Figure 3b) to shift the wavelength results. The wavelength master curves versus shifted annealing time as a function of film thickness are summarized in Figure 4.

**Stress Relaxation Modulus.** Figure 5 summarizes the PS modulus master curves based on the wavelength master curves presented in Figure 4. With the exception of the 642 nm PS film, eq 11 was used to infer the PS modulus for all the film thicknesses. Because the 642 nm thick sample is intermediate between the geometrically unconfined and confined limits, eq 11 did not provide an accurate description of the stress relaxation modulus. Within this intermediate region, the relationship between wavelength and PS film thickness is extremely sensitive to the film thickness. For the 642 nm thick PS film, we determined that  $g = 2(kh_{PS})^{-7/5}$ , which leads to the following relationship.

$$E_{PS}(t, T, kh_{PS} \approx 1) = \frac{E_{AI}}{29(1 - \nu_{AI}^2)} \left(\frac{h_{PS}}{h_{AI}}\right)^{7/5} (k(t, T)h_{AI})^{22/5} \quad (13)$$

With the exception of the 74 nm thick PS film, Figure 5 suggests that the stress relaxation modulus for PS is nearly independent of the film thicknesses investigated when we use eq 11 and eq 13 to correct for stiffness effects. Hence, we used a single power law stress relaxation function to fit all the results<sup>36</sup>

$$E_{PS}(t, T) = E_{PS,p} \left( \frac{1}{1 + (t/\tau)} \right)^\beta \quad (14)$$

where  $E_{PS,p}$  is the plateau modulus,  $\tau$  is the terminal relaxation time, and  $\beta$  is the power-law exponent. Using eq 14, the best fit of the results corresponded to:  $E_{PS,p} = 7.3 \times 10^5 \text{ N/m}^2$ ,  $\tau = 6500 \text{ s}$  and  $\beta = 0.66$ . These extrapolated values are in good agreement with the bulk rheology<sup>37</sup> and literature values<sup>38</sup>. As discussed previously, a plateau modulus was observed at short annealing times up to the point of the terminal relaxation time. Within this range of time-scale that is less the terminal relaxation time, the wrinkling process can be described as a primarily elastic response. Past the terminal relaxation time, a terminal flow regime was reached, characterized by significant changes in the modulus of PS. Within this time scale, the mechanical properties and the resultant wrinkling process are now dominated primarily by the viscous response of the polymer as demonstrated recently by Vanderparre and co-workers.<sup>24</sup> Specifically, the polymer stress relaxed in response to the applied thermal strain, and the origin of this response is related to the transient nature of the physical cross-links between the polymer chains. Past the terminal relaxation time, these temporary cross-links can slip past each other and leads to stress relaxation of the polymer. In relation to thermal

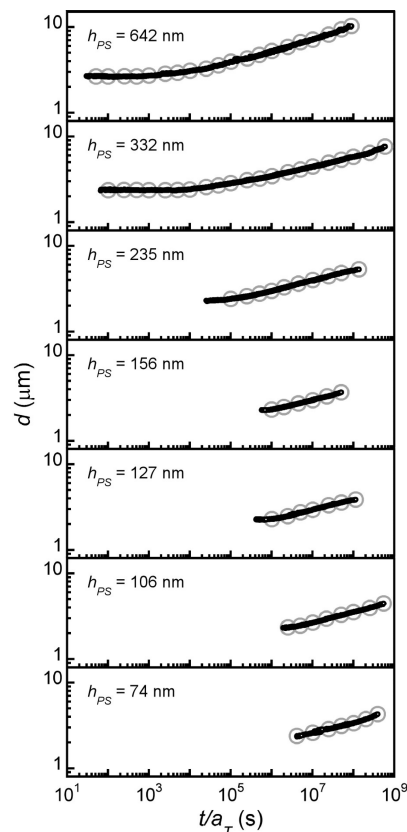


**Figure 4.** Wavelength ( $d$ ) master curves for PS thin films as a function of shifted annealing time ( $t/a_T$ ). The open symbols represent selected time points from the entire data set shown by the filled symbols. The error bars are smaller than the symbol size.

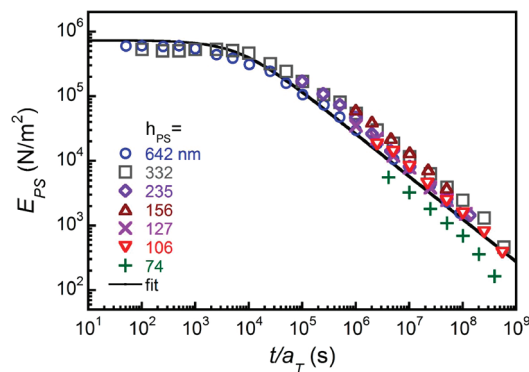


**Figure 5.** Summary of modulus ( $E_{PS}$ ) master curves for PS thin films as a function of shifted annealing time ( $t/a_T$ ). The data points used to determine the modulus values are taken from the selected wavelength vs time points as shown in Figure 4. The reference temperature used for the time–temperature superposition shifting was  $120^\circ\text{C}$ .

wrinkling, the wrinkling process past the terminal relaxation time can be characterized as a viscous wrinkling process. Similar to the terminal relaxation time measured from bulk rheology, this time-scale measured from thermal wrinkling describes the transition point between a primarily elastic versus a primarily viscous wrinkling process. By combining eqs 11 and 14 and relating the terminal relaxation time ( $\tau = \eta_{PS}/E_{PS,p}$ ) as the ratio of the viscous response (shear viscosity,  $\eta_{PS}$ ) to the elastic response (plateau modulus,  $E_{PS,p}$ ), the following wavelength evolution

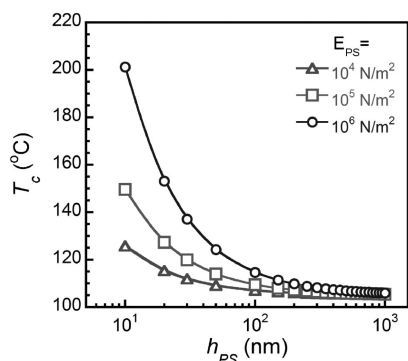


**Figure 6.** Predicted critical annealing temperature for wrinkling ( $T_c$ ) as a function of PS film thickness and modulus. The Al film thickness is assumed to be constant at 20 nm. The PS layer is assumed to be confined and incompressible.

relationship is developed

$$d(t, T, kh_{PS} \rightarrow 0) = \left(\frac{2\pi}{k}\right) \\ = 2\pi(h_{PS}h_{Al})^{1/2} \left(\frac{1}{18(1-\nu_{Al}^2)} \frac{E_{Al}}{E_{PS,p}}\right)^{1/6} \left(1 + \left(\frac{E_{PS,p}}{\eta_{PS}}\right)t\right)^{11/100} \quad (15)$$

An interesting aspect of eq 15 is that it has a similar form as developed by Vandeparre and co-workers<sup>24</sup> although the exact expressions are unique because of the specific polystyrene system. Specifically, Vandeparre and co-workers have considered the wrinkling behavior of the polystyrene layer to be purely viscous driven, whereas we consider our polystyrene layer to be viscoelastic because its molecular mass is well-above the entanglement limit.

One last comment we would like to make about Figure 5 concerns the stress relaxation modulus of the 74 nm thick PS film. This set of data did not match the stress relaxation function obtained for other film thicknesses. From the limited data points, a different stress relaxation function with different fitting constants is needed to describe the response. It would appear that the terminal relaxation time should be shorter; the origin of this deviation warrants further investigation in the future. Due to the resolution limitation of the SALS instrument, it is beyond the scope of this work. However, we can estimate the critical annealing temperature for wrinkling as a function of PS film thickness. For a PS thin film that is considered as confined and incompressible, the critical wrinkling strain is defined by eq 9. By equating eq 1 with eq 9, we can estimate critical annealing temperature for wrinkling ( $T_c$ ) as a function of PS film thickness

$$T_c = T_o + \frac{1}{4(\alpha_{Al} - \alpha_{Si})} \left(\frac{h_{Al}}{h_{PS}}\right) \left(3E_{PS} \frac{1 - \nu_{Al}^2}{E_{Al}}\right)^{1/3} \quad (16)$$

where  $T_o$  is the reference temperature, which we assume to be the glass transition of PS. The predictions as a function of PS film thickness and modulus (from  $1 \times 10^4$  N/m<sup>2</sup> to  $1 \times 10^6$  N/m<sup>2</sup>) for a constant Al film thickness ( $h_{Al} = 20$  nm) are summarized in Figure 6. The results demonstrate that the critical wrinkling temperature is inversely proportional to the thickness ratio ( $h_{PS}/h_{Al}$ ). Therefore, the resistance for thermal wrinkling increases with decreasing thickness ratio. In other words, it becomes more difficult

to measure the viscoelastic properties of the PS thin film without resorting to higher annealing temperatures or longer annealing times. One possible solution is to maintain a constant value of the thickness ratio at all PS film thicknesses. The challenge in this solution lies in ensuring that the mechanical properties of the Al thin film are constant with film thickness.

#### 4. CONCLUSION

This work demonstrates that thermal wrinkling can be used to measure the stress-relaxation modulus of polymer thin films confined by both a substrate and superstrate. With the appropriate buckling mechanics model, the history dependent modulus can be appropriately determined as a function of the polymer thin film thickness. Because the driving force for thermal wrinkling is related to the development of a critical thermal strain, the annealing temperature must be sufficiently high to cause this instability as the temperature-dependent modulus of the polymer film is the limiting factor. Hence, we expect that the thermal wrinkling approach is capable of accurately measuring the rubbery plateau and terminal flow region of a viscoelastic polymer film. However, it would be difficult to measure the properties near the glass-transition region.

From the evolution of the wrinkle wavelength with annealing time, we observed two distinct regions of the wrinkling process that are influenced by the viscoelastic properties of the PS layer. For annealing times shorter than the terminal relaxation time, the thermal wrinkles are stable over this time-scale and can be considered as an elastic wrinkling process because the PS viscoelastic properties can be described primarily by its plateau modulus. For annealing times longer than the terminal time, the viscous properties of the PS determine the wrinkling process as characterized by the wavelength increase with time. Future work will involve using thermal wrinkling to explore the role of ultrathin film thickness, as well as molecular weight on the viscoelastic properties of the polymer layer. Instead of light scattering, we can potentially use optical profilometry as a high-throughput, high-resolution measurement tool to monitor the evolution of the thermal wrinkles, which can also facilitate quantitative measurement of the evolution of the wrinkle amplitude.

Finally, the results of this work are also beneficial to understanding the temporal and thermal evolution of surface wrinkles, which would be especially useful for applications of these materials as patterned surfaces. Since the morphology of these surfaces evolves, a specific pattern length scale can be selected with the appropriate selection of thermal processing time-scale based on the viscoelastic properties and film geometry employed.

#### ■ ASSOCIATED CONTENT

**S Supporting Information.** Discussion of the stiffness function for compressible and incompressible polymer layer, and bulk rheology experiments of polystyrene (PDF). This material is available free of charge via the Internet at <http://pubs.acs.org>.

#### ■ AUTHOR INFORMATION

##### Corresponding Author

\*E-mail: [chris.stafford@nist.gov](mailto:chris.stafford@nist.gov).

#### ■ ACKNOWLEDGMENT

E.P.C. acknowledges the National Research Council for financial support. The authors thank Dr. Wen-Li Wu, Dr. Jun Young Chung

Dr. Peter M. Johnson, Dr. Jack F. Douglas, Dr. Kenneth L. Kearns, and Dr. Kathryn L. Beers for insightful discussions. The authors also thank Dr. Denis Pristinski for technical assistance with the SALS instrument.

## REFERENCES

- (1) Goldblatt, R. D. A.; Anand, M. B.; Barth, E. P.; Biery, G. A.; Chen, Z. G.; Cohen, S.; Connolly, J. B.; Cowley, A.; Dalton, T.; Das, S. K.; Davis, C. R.; Deutsch, A.; DeWan, C.; Edelstein, D. C.; Emmi, P. A.; Faltermeier, C. G.; Fitzsimmons, J. A.; Hedrick, J.; Heidenreich, J. E.; Hu, C. K.; Hummel, J. P.; Jones, P.; Kaltalioglu, E.; Kastenmeier, B. E.; Krishnan, M.; Landers, W. F.; Liniger, E.; Liu, J.; Lustig, N. E.; Malhotra, S.; Manger, D. K.; McGahay, V.; Mih, R.; Nye, H. A.; Purushothaman, S.; Rathore, H. A.; Seo, S. C.; Shaw, T. M.; Simon, A. H.; Spooner, T. A.; Stetter, M.; Wachnik, R. A.; Ryan, J. G., . *Proceedings of the IEEE 2000 International Interconnect Technology Conference*; Burlingame, CA, June 5–7, 2000 ; IEEE: Piscataway, NJ, 2000; pp 261–263.
- (2) Kim, C.; Facchetti, A.; Marks, T. J. *Science* **2007**, *318*, 76–80.
- (3) Gotsmann, B.; Knoll, A. W.; Pratt, R.; Frommer, J.; Hedrick, J. L.; Duerig, U. *Adv. Mater.* **2010**, *20*, 1–9.
- (4) Hart, S. D.; Maskaly, G. R.; Temelkuran, B.; Prideaux, P. H.; Joannopoulos, J. D.; Fink, Y. *Science* **2002**, *296*, 510–513.
- (5) Schulz, U.; Kaiser, N. *Prog. Surf. Sci.* **2006**, *81*, 387–401.
- (6) Farhat, T. R.; Hammond, P. T. *Adv. Funct. Mater.* **2005**, *15* (6), 945–954.
- (7) Reiter, G. *Macromolecules* **1994**, *27* (11), 3046–3052.
- (8) Cho, Y.-K.; Watanabe, H.; Granick, S. J. *Chem. Phys.* **1999**, *110* (19), 9688–9696.
- (9) Tsui, O. K. C.; Wang, X. P.; Ho, J. Y. L.; Ng, T. K.; Xiao, X. *Macromolecules* **2000**, *33*, 4198–4204.
- (10) O'Connell, P. A.; McKenna, G. B. *Science* **2005**, *307*, 1760–1766.
- (11) Hillman, A. R.; Efimov, I.; Ryder, K. S. J. *Am. Chem. Soc.* **2005**, *127* (47), 16611–16620.
- (12) Barbero, D. R.; Steiner, U. *Phys. Rev. Lett.* **2009**, *102*, 248303.
- (13) Chan, E. P.; Page, K. A.; Im, S. H.; Patton, D. L.; Huang, R.; Stafford, C. M. *Soft Matter* **2009**, *5* (23), 4638–4641.
- (14) Kim, J.; Lee, H. H. *J. Polym. Sci. B: Polym. Phys.* **2001**, *39* (11), 1122–1128.
- (15) Sharp, J. S.; Vader, D.; Forrest, J. A.; Smith, M. I.; Khomenko, M.; Dalnoki-Veress, K. *Eur. Phys. J. E* **2006**, *19* (4), 423–432.
- (16) Yoo, P. J.; Lee, H. H. *Phys. Rev. Lett.* **2003**, *91* (15), 154502.
- (17) Yoo, P. J.; Suh, K. Y.; Kang, H.; Lee, H. H. *Phys. Rev. Lett.* **2004**, *93* (3), 034301 (1–4).
- (18) Zhang, H.; Okayasu, T.; Bucknall, D. G. *Eur. Polym. J.* **2004**, *40*, 981–986.
- (19) Huang, Z. Y.; Hong, W.; Suo, Z. *J. Mech. Phys. Solids* **2005**, *53*, 2101–2118.
- (20) Yoo, P. J.; Lee, H. H. *Macromolecules* **2005**, *38* (7), 2820–2831.
- (21) Vandeparre, H.; Leopoldes, J.; Poulard, C.; Desprez, S.; Derue, G.; Gay, C.; Damman, P. *Phys. Rev. Lett.* **2007**, *99*, 188302.
- (22) Hendricks, T. R.; Lee, I. *Nano Lett.* **2007**, *7*, 372–379.
- (23) Hendricks, T. R.; Wang, W.; Lee, I. *Soft Matter* **2010**, *6*, 3701–3706.
- (24) Vandeparre, H.; Gabriele, S.; Brau, F.; Gay, C.; Parker, K. K.; Damman, P. *Soft Matter* **2010**, *6*, 5751–5756.
- (25) Stover, J. C. *Optical Scattering: Measure and Analysis*, 2nd ed.; SPIE Optical Engineering Press: Bellingham, WA, 1995.
- (26) Hsueh, C.-H.; Lee, S.; Lin, H.-Y. *Composites B* **2006**, *37*, 1–9.
- (27) Volinsky, A. A.; Moody, N. R.; Gerberich, W. W. *Acta Mater.* **2002**, *50*, 441–466.
- (28) Allen, H. G., *Analysis and Design of Structural Sandwich Panels*; Pergamon: New York, 1969.
- (29) Chen, X.; Hutchinson, J. W. *J. Appl. Mech.* **2004**, *71*, 597–603.
- (30) Stafford, C. M.; Vogt, B. D.; Harrison, C. M.; Julthongpiput, D.; Huang, R. *Macromolecules* **2006**, *39* (15), 5095–5099.
- (31) Chen, X.; Hutchinson, J. W. *Scr. Mater.* **2003**, *50*, 797–801.
- (32) Huang, R.; Im, S. H. *Phys. Rev. E* **2006**, *74*, 026214.
- (33) Young, R. J.; Lovell, P. A., *Introduction to Polymers*, 2nd ed.; CRC Press: Boca Raton, FL, 1991; p 443.
- (34) Williams, M. L.; Landel, R. F.; Ferry, J. D. *J. Am. Chem. Soc.* **1955**, *77* (14), 3701–3707.
- (35) Plazek, D. J. *J. Phys. Chem.* **1965**, *69* (10), 3480–3487.
- (36) Friedrich, C.; Braun, H. *Rheol. Acta* **1992**, *31*, 309–322.
- (37) Please refer to the Supporting Information, Figure S1.
- (38) Knoff, W. F.; Hopkins, I. L.; Tobolsky, A. V. *Macromolecules* **1971**, *4* (6), 750–754.
- (39) Wallace, W. E.; van Zanten, J. H.; Wu, W. L. *Phys. Rev. E* **1995**, *52* (4), R3329–R3332.
- (40) Kim, M. T. *Thin Solid Films* **1996**, *283*, 12–16.